



**National
Oceanography Centre**

NATURAL ENVIRONMENT RESEARCH COUNCIL

Coastal & Open Ocean Surface Currents Mission Study: Wavemill Product Assessment (WaPA)

Invitation to Tender AO/1-7051/12/NL/AF

**WP1000 ATI SAR surface current
velocity review (D1)**

Christine Gommenginger (NOC)

National Oceanography Centre

14 October 2013

Version 1.1

© The Copyright of this document is the property of National Oceanography Centre (NOC). It is supplied on the express terms that it be treated as confidential, and may not be copied, or disclosed, to any third party, except as defined in the contract, or unless authorised by NOC in writing.

**National Oceanography Centre, Southampton
European Way, Southampton
SO14 3ZH, United Kingdom
Tel: +44 (0)23 80596413 Fax: +44 (0)23 80596400**



DOCUMENT SIGNATURE TABLE

	Name	Institution	Signature	Date
Prepared by	C. Gommenginger	NOC		05/04/2013
Revised by	C. Gommenginger	NOC		14/10/2013
Authorised by	C. Gommenginger	NOC		14/10/2013



DISSEMINATION

To:	Means
Christopher Buck, ESA	Christopher.Buck@esa.int
David Cotton, SATOC Ltd	d.cotton@satoc.eu
Jose Marquez, Starlab	jose.marquez@starlab.es
Marco Caparrini, Starlab	marco.caparrini@starlab.es
Bertrand Chapron, Ifremer	Bertrand.Chapron@ifremer.fr
Geoff Burbidge, EADS Astrium	geoff.burbidge@astrium.eads.net



ISSUE RECORD

Issue No.	Issue Date	Sections affected	Relevant information
V1.0	05/04/2013	-	First draft
V1.1	14/10/2013	Various	Changes in response to ESA comments & input from WaPA team



TABLE OF CONTENTS

Document signature table	2
Dissemination.....	3
Issue record.....	4
Table of contents	5
1 Purpose of this document.....	7
2 Content of this document.....	7
3 Overview of key publications	8
3.1 Goldstein & Zebker (1987): Interferometric Radar Measurement of Ocean Surface Currents.....	8
3.2 Graber, Thompson & Carande (1996): Ocean surface features and currents measured with SAR interferometry and HF radar.....	9
3.3 Romeiser & Thompson (2000): Numerical study on the ATI radar imaging mechanism of oceanic surface currents.....	10
3.4 Frasier & Camps (2001): Dual-beam interferometry for ocean surface current vector mapping.....	11
3.5 KoRIOLiS (2002): Study on Concepts for Radar Interferometry from satellites for Ocean (and Land) Applications	11
3.6 The BNSC NEWTON study, 2002: Along Track SAR Interferometry for Ocean Currents and Swell	12
3.7 Siegmund <i>et al.</i> (2004): First demonstration of surface currents imaged by hybrid along- and cross-track interferometric SAR	12
3.8 Romeiser <i>et al.</i> (2005b): Current measurements by SAR along-track interferometry from a space shuttle	14
3.9 Toporkov <i>et al.</i> (2005): Sea surface velocity vector retrieval using dual-beam interferometry: First demonstration	14
3.10 Sletten (2006): An analysis of gradient-induced distortion in ATI-SAR imagery of surface currents.....	15
3.11 Romeiser <i>et al.</i> (2010a): First Analysis of TerraSAR-X Along-Track InSAR-Derived Current Fields.....	15
3.12 Kumagae <i>et al.</i> (2011): Sea Surface Current Measurement with Ku-Band SAR Along- Track Interferometry.....	17
3.13 Toporkov <i>et al.</i> (2011): Surface Velocity Profiles in a Vessel's Turbulent Wake Observed by a Dual-Beam Along-Track Interferometric SAR.....	17
3.14 Hansen <i>et al.</i> (2012): Simulation of radar backscatter and Doppler shifts of wave- current interaction in the presence of strong tidal current.....	17
4 Literature review Synthesis.....	19
4.1 Interferometric SAR systems	19
4.2 Experimental sites, environmental conditions and means of validation.....	20
4.3 Errors and mitigation strategies.....	21
4.3.1 Attitude and navigation errors.....	21
4.3.2 Errors specific to squinted systems.....	21
4.3.3 Long swell waves.....	22
4.3.4 Wind drift.....	23



4.4	Theoretical modelling and model performance.....	23
5	Implications for a future spaceborne Wavemill mission.....	25
6	Implications for Wavemill ocean current products.....	26
7	Conclusions.....	27
Annex A: Summary table for key publications relevant to ATI SAR ocean currents		28
8	List of Acronyms.....	36
9	Bibliography.....	37



1 PURPOSE OF THIS DOCUMENT

This document represents the Technical Note (D1) for WP1000 of the Coastal & Open Ocean Surface Currents Mission Study: Wavemill Product Assessment (WaPA) study, awarded in response to ESTEC Invitation to Tender AO/1-7051/12/NL/AF.

The objectives of WP1000 are to:

- perform an in-depth literature review of past experimental and theoretical modelling studies relating to Along-Track Interferometric (ATI) SAR for the retrieval of ocean current products and other parameters.
- identify key geophysical phenomena affecting ATI SAR surface current retrieval, review theoretical models proposed to represent the microwave scattering and determine the capability of these models to reproduce experimental results.
- document past experimental results in terms of the environmental conditions in which the measurements took place, what ground-truth was available for validation and the basic parameters of the radar systems.
- elaborate the implications of previous ATI SAR studies for a spaceborne Wavemill mission and the Wavemill scientific product requirements, accounting for the way performance may be affected when transferring from a 1D ATI to a Wavemill 2D system.

We note that this review is focused primarily on the literature pertaining to the retrieval of ocean currents with ATI SAR. However, some relevant findings are also found elsewhere, for example regarding the effects of ocean waves and wind in other microwave techniques.

Thus, there exists for example an extensive literature on the retrieval of wind, waves and currents from “conventional” SAR (i.e. single-antenna systems), within which some publications provide interesting insight about the scattering responsible for the signals contributing to SAR, and indeed ATI SAR, measurements. But, since it was not possible within the scope of this task to include also an extensive review of the large body of work on SAR over oceans, we were able to consider only a few of these key references in this report.

2 CONTENT OF THIS DOCUMENT

This review is structured as follows.

Section 3 gives a brief summary of major publications relevant to ATI SAR current retrieval, reporting the methods, datasets and main results from each study. Only publications, which contribute original methods and insight, are highlighted in this way, other papers being simply cited in the general text. This approach makes it possible to condense contemporaneous publications by members of the same group into a smaller number of contributions, and retains some trace of the broader historical evolution of the knowledge, instruments, processing and correction methods. For ease of reference, technical details from key publications are also summarised in the Summary table provided in Annex A.



Section 4 provides a synthesis of the outcome from the literature review regarding the specific points raised in Section 1, namely:

- The basic parameters of the radar systems
- The experimental sites, environmental conditions and means of validation used
- The errors and mitigation strategies
- Theoretical modelling and model performance

Finally, Section 5 draws up the implications following this review for the design and development of a spaceborne Wavemill mission.

3 OVERVIEW OF KEY PUBLICATIONS

This section provides an overview of activities and findings in key publications relevant to ATI retrieval of ocean currents. Technical details from these key publications are also summarised in the Summary table provided in Annex A.

3.1 Goldstein & Zebker (1987): Interferometric Radar Measurement of Ocean Surface Currents

Goldstein & Zebker (1987) offer the first example of ocean surface current measurements with an airborne ATI SAR operating at L-band. Quantitative estimates of one component of the ocean current are obtained over San Francisco Bay shortly after maximum tidal flow (2.6 m/s) and for two coastal eddies a few km in diameter with magnitude 1.6 m/s and 0.8 m/s. Uncorrected aircraft yaw error (~ 0.01 deg) is associated with a velocity error of 4 cm/s. Environmental conditions were light, described as “relatively smooth with little swell”. The ATI derived velocity is attributed to the sum of the line-of-sight components of the current, Bragg waves and the orbital velocity of swell waves. Swell is neglected here because no waves are visible in the (fairly) high-resolution images (60 x 60 meters). Although the Bragg waves phase velocity of 0.5 m/s is above the instrument threshold, there is no large difference in retrieved velocity between ocean and land, leading the authors to conclude that “each resolution element must contain nearly equal Bragg components travelling both towards and away from the radar”.

In another airborne experiment with the same system, Goldstein *et al.* (1989), validate ATI currents against freely drifting buoys, which consisted of drifting pieces of plywood 1.2 m long by 0.6 m wide by 2 cm deep designed to capture the very-near-surface current seen by the radar, and were positioned by Loran-C. Mitigating the effect of swell on the ATI currents by first averaging phase to 100 by 100 metres, the two estimates of surface current are linearly related with a slope of $1.12 + 0.18$ (95% confidence limits), have little bias (2.2 cm/s) and a rms error of 12 cm/s.

Marom *et al.* (1990), report another airborne experiment, again with the same instrument, but focussing instead on ATI measurements of bimodal ocean wave spectra over Monterey Bay. Wave spectra are computed for ATI velocity images of resolution 6m (range) by 12m (azimuth) and compared with in situ data from a wave pressure sensor, with very good agreement. Environmental conditions were light, with low wind (< 2 m/s) and



low sea state (SWH < 0.6m). The waves direction of propagation during the experiment was close to the radar line-of-sight, making conditions ideal for SAR imaging (minimum distortion due to velocity bunching). The authors note that waves are more clearly visible in ATI than SAR amplitude images. It is stated that ocean waves were still visible in an orthogonal flight path for ATI but not for SAR, leading to the conclusion that range orientation is “probably not essential for obtaining clear ATI images of ocean waves”. ATI velocity observed over inland water - where waves are generated by local wind only - matches the phase velocity of the upwind resonant waves (~ 0.5 m/s) calculated from linear wave theory.

3.2 Graber, Thompson & Carande (1996): Ocean surface features and currents measured with SAR interferometry and HF radar

Graber *et al.* (1996), present the first comprehensive airborne ATI validation campaign backed by a unusually complete set of ground-truth measurements and an advanced modelling component. Airborne ATI data were obtained during the 1993 High-Resolution Remote Sensing Experiment (High-Res) over the inshore edge of the Gulf Stream North Wall off the coast of Cape Hatteras. ATI ocean currents are validated against data from HF radar (1km resolution), two research vessels (ADCP current profiles) and buoys providing standard meteorological data, directional wave spectra and vector current meter data at 10 meters.

The paper proposes two methods to eliminate the effect of surface wave motion: a) using some knowledge of local wind and wave field and a microwave scattering model (Thompson (1989); Thompson *et al.* (1991)); b) using a few in situ measurements of currents at different ranges in the INSAR image. In the absence of a functional GPS system during the flights, the paper also puts forward a way to mitigate range-dependent biases in phase - induced by poorly known altitude and mis-alignment of the platform velocity vector with the AT baseline - by determining the mean range-dependent phase trends and force the phase to zero over regions of negligible height changes and zero horizontal velocity (e.g. Outer Banks).

Modeling of ATI currents is based on the Doppler spectrum model by Thompson (1989), and wind vector and wave spectra from in situ data. Presenting the modeled Doppler velocities as a function of incidence (Figure 1), the authors highlight the slower decrease with incidence of the Bragg phase velocity, especially at smaller incidence angles, compared to curves that account also for longer ocean waves, and the near-similar behavior with incidence of the curves relating to slightly different wind directions, which are thus equivalent to within a scaling constant. A wind drift velocity, usually estimated to be about 3% of the 10 meters wind speed, contributes an additional constant offset to the mean Doppler velocities shown in Figure 1. Small uncertainties in wind drift velocity, wind direction and/or the spreading width of the surface wave spectrum can lead to differences in mean Doppler velocity as a function of range of the order of 0.2 m/s.

Overall, the agreement between ATI and HF radar (both reduced to 1km resolution) is very good (within 0.11 m/s) and ATI SAR is found able to detect abrupt changes in current speed and direction associated with collision of water masses, making 2D current maps



from ATI very beneficial for the study of dynamics of small-scale surface features in regions of strong current divergences or shears.

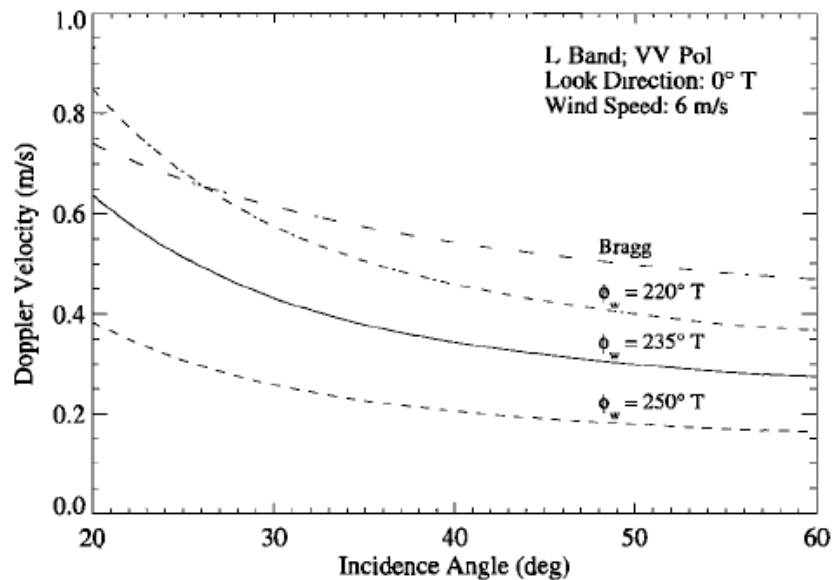


Figure 1: Computed L-band Doppler velocities as a function of incidence angle for VV polarisation and a radar look direction of 0 deg. All computations are for 6 m/s winds. The curves labeled by Φ_w show the computed results for the winds from the indicated direction. The curve labelled “Bragg” shows the dependence of the Bragg phase speed as a function of incidence angle (From: Graber *et al.* (1996))

3.3 Romeiser & Thompson (2000): Numerical study on the ATI radar imaging mechanism of oceanic surface currents

This paper presents a new model to compute the Doppler spectrum and ATI SAR signature of the radar return from the ocean surface. The Doppler spectrum of the radar return from the ocean surface, as detected by coherent microwave radars, reflects the distribution of the line-of-sight velocity of the scatterers, weighted by their contributions to the backscattered power. Based on Bragg scattering theory in a composite surface model approach, the model accounts for contributions to Doppler velocities by Bragg components and, via higher order effects, by the orbital motions of ocean waves which can be considered long compared to the Bragg scattering facets and thus modulate the backscattered signal in amplitude and frequency.

The model is compared against the established numerically-intensive model by Thompson (1989), which was itself successfully validated against observations at L- and Ku-band (Thompson *et al.* (1991)) and is used here as reference. Evidence of validation against Thompson (1989), consists of comparisons of the normalised Doppler spectra at L-band for an incidence angle of 30 degrees and three values of wind speed (3,6 and 12 m/s) in the absence of current. The new model provides an efficient solution that speeds up computation by one to two orders of magnitude.



The rest of the paper deals with purely numerical simulations (without recourse to observations for further validation) with the new model coupled with surface wave spectrum modulation by currents according to the weak hydrodynamic interaction theory by Romeiser & Alpers (1997). The simulations determine the sensitivity of ATI current measurements to various environmental and radar parameters, predicting that best results can be expected for ATI systems operated at high microwave frequencies (e.g. X-band), high incidence angles (e.g. 60 deg), low platform altitude/speed ratio and vertical polarisation.

3.4 Frasier & Camps (2001): Dual-beam interferometry for ocean surface current vector mapping

This paper presents a dual-beam along-track interferometer system to provide spatially resolved surface velocity vectors with a single-pass. The system comprises a pair of interferometric beams, one squinted forward, the other squinted aft, the instrument being sensitive to the line of sight velocity in the direction of each beam. The means to estimate the response of a squinted ATI-SAR, including the effect of platform attitude and velocity errors, is presented, leading to the recommendation for moderate squint angles (45 deg) and larger incidence angles. The paper points out the potential additional application to wind scatterometry with the same instrument if the squint angle is chosen large. Estimates of the degree of polarization mixing (to be avoided) are given for different incidences and squint angles. Finally, the authors report the azimuthal displacement of interferometric phase by moving surfaces identical to that seen in conventional SAR, finding that such displacement can bias the estimated surface velocity.

The DBI concept is made a reality in Frasier *et al.* (2001), who give details of a prototype pod-based dual-beam interferometric radar system developed by University of Massachusetts (UMass). Junek *et al.* (2003), and Farquharson *et al.* (2004) both present preliminary data collected in the airborne trials of the UMass system (characterised by incidence angles around 70 deg and squint angle of ± 20 deg) over Charlotte Harbour, Florida.

3.5 KoRIOLIS (2002): Study on Concepts for Radar Interferometry from satellites for Ocean (and Land) Applications

The KoRIOLIS study on Concepts for Radar Interferometry from satellites for Ocean (and Land) Applications provides an in-depth review of along-track, across-track and hybrid interferometric SAR for the measurement of ocean currents and waves. Funded by the German Federal Ministry of Research, KoRIOLIS contains contributions from leading German specialists in ocean remote sensing with SAR (R. Romeiser, J. Schulz-Stellenfleth, S. Lehner, M. Schwäbisch, R. Siegmund) and by Donald R. Thompson from Johns Hopkins University Applied Physics Laboratory, USA.

KoRIOLIS represents a state of the art in interferometric SAR techniques including useful material on fundamental principles and capabilities of interferometric SAR techniques, and discussions of technical issues (e.g. impact of hybrid interferometric baselines) and possible concepts for spaceborne implementation. assessment of the at that time



3.6 The BNSC NEWTON study, 2002: Along Track SAR Interferometry for Ocean Currents and Swell

This study, commissioned in 2000 by the British National Space Centre, investigated the capability of ATI SAR for ocean current and swell (Anderson *et al.* (2003a); Anderson *et al.* (2003b)). After a review of the nature, magnitude and variability of ocean currents and ocean surface motions in the open ocean and coastal regions, the study analyses ATI SAR data obtained from the JPL airborne AIRSAR system at L-band and C-band in two regions: near Hawaii at the northern tip of Big Island and south-west of Japan in the Kuroshio jet area.

ATI phase and velocity were modelled using a composite model after method of Romeiser & Thompson (2000). Input to the scattering model consisted of directional wave spectra from the WAM 3rd generation wave model coupled to ocean currents from the OCCAM ¼ deg ocean model and the HOPE local tide model, and wind forcing from the ¼ deg ECMWF operational model. The scattering model was able to account for tilt and hydrodynamic modulation, and showed that tilt effects are important, particularly at low incidence angles. Despite severe degradation of the ATI phase data due to poor compensation for aircraft attitude during the flights, the modelled ATI currents successfully reproduced the magnitude and variability of large-scale tidal and geostrophic currents seen in the AIRSAR data. Smaller features, linked to eddies and wind sheltering by orographic effects in the lee of the tip of Hawaii island, could not be captured, it is presumed because of the relatively coarse resolution of the models providing wind, wave and current input to the scattering model.

3.7 Siegmund *et al.* (2004): First demonstration of surface currents imaged by hybrid along- and cross-track interferometric SAR

This paper presents the first example of an hybrid Interferometric SAR used in an airborne experiment to simultaneously measure elevation and ocean currents. The airborne X-band system was deployed over the (German) Wadden Sea at the mouth of the estuary of the Weser river near Bremenhaven during fairly rough wind conditions (8-10 m/s, according to a local coastal met station). The airborne flights took place 30 minutes before low tide, in an area where maximum current is around 1.2 m/s. Two anti-parallel flights taken 10 minutes apart and aligned with the dominant wind direction provide the means of investigating the phase difference over land and water when looking up- and down-wind.

A geometrical model is proposed to compute the hybrid Interferometric phase, revealing the ambiguity in differentiating phase effects from elevation and from radial velocity in hybrid systems. The cross-track baseline in hybrid systems also introduces mis-registration of targets in azimuth as seen by the two antennas, which shows up as ghosting in the final images. This mis-registration increases with increasing radial velocity of the target, and, due to the squint angle, leads to a bias in phase. The effect is linearly related to R/V (with V the velocity of the platform) and is therefore worse for airborne systems.

No correction is applied for orbital velocity of waves, which is thought negligible due to the short fetch, but both wind drift (0.3 m/s) and Bragg scatterers phase velocity (0.2 m/s)



components are removed. The paper presents realistic retrieved currents and height maps, thus providing a demonstration of combined measurement of terrain height over land and currents over water surfaces (Figure 2).

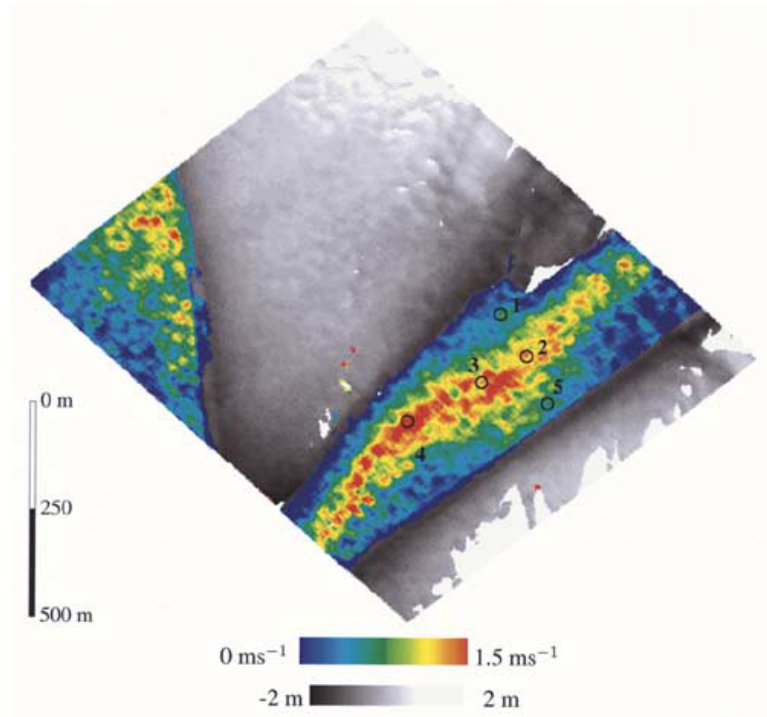


Figure 2: Terrain height and ground range velocity obtained from two anti-parallel flights taken 10 minutes apart in the estuary mouth of the Weser river in the German Bight (from: Siegmund et al. (2004))

Nevertheless, when comparing the airborne retrieved currents with estimates from the numerical hydrodynamic model, the airborne system provides good estimates of low currents but overestimate the maximum current by up to 0.4 m/s, a problem attributed to the mis-registration of moving targets linked to the hybrid nature of the interferometric baseline.



3.8 Romeiser *et al.* (2005b): Current measurements by SAR along-track interferometry from a space shuttle

This paper presents current retrieval from interferometric SAR data from the Shuttle Radar Topography Mission (SRTM). Designed for digital elevation mapping, the SRTM X-band Interferometric SAR system features a large across-track baseline as well as a small along-track baseline (3.5m). Although the sensitivity of the SRTM ATI phase to current variations is poor (1m/s ~ 10deg in phase), the study presents compelling current maps for SRTM over the Dutch Wadden Sea, which are compared with output from a hydrodynamic model (KUSTWAD). For scales 1 km and longer, the correlation between SRTM and the model is greater than 0.5 and the SRTM rms error is 0.24 m/s. Simulated SRTM phase images are produced with the model by Romeiser & Thompson (2000) based on input from the KUSTWAD hydrodynamic model and a 5m/s westerly wind (from local weather observations). Wave-current interactions and non-linear scattering effects are neglected, and the surface wave spectrum is adjusted at each grid point to be in equilibrium with local effective wind (i.e. wind vector minus local current vector). Differences between ATI modelled currents and KUSTWAD currents are dominated by scales larger than 10km, and are linked to residual errors due to SRTM mast oscillations.

Romeiser *et al.* (2007), applied a similar approach to one SRTM scene over the Elbe River where river currents could be retrieved. The authors note that in most cases (105 scenes examined), meaningful currents in rivers could not be retrieved due to low signals levels and low coherence, and the strong sensitivity of phase to topographic height of surrounding land. The height sensitivity of the phase is highlighted as a fundamental disadvantage of combined along-track/cross-track design for ocean and river applications. Similarly, no correction is applied for wave contributions as the numerical InSAR imaging model was not adapted to the specific requirements of river simulations (modified parameterisation of equilibrium wave spectrum and improved representation of modulation linked to refraction, reflection and dissipation near shallow regions, beaches and steep river banks)

3.9 Toporkov *et al.* (2005): Sea surface velocity vector retrieval using dual-beam interferometry: First demonstration

Reporting on the first scientifically-motivated airborne campaign of the UMass dual-beam interferometer (DBI; see Frasier & Camps (2001)), this paper demonstrates the capability of the squinted ATI-SAR DBI to retrieve ocean current vector from single-pass data. The paper provides in-depth analyses of the preliminary results over the Florida barrier islands that are also presented in Toporkov *et al.* (2004) and Perkovic *et al.* (2005).

Airborne measurements of currents over the highly dynamic inlets of the Florida barrier islands are compared against tidal predictions from the NOAA National Ocean Service (NOS). High-rate data from on-board GPS/DGPS inertial system serve to correct for position and attitude effects. No correction for surface wave motion is attempted, although the velocity contribution of surface waves is estimated around 0.5 m/s and identified as the main cause of the observed discrepancies with the NOS currents. The paper uses variable spatial resolution, which enables it to retain high resolution (6 x 6 metres) in areas of high coherence (e.g. near inlets), while averaging phase (down to 120 x 120 m) in areas of



increased noise (e.g. far range). The intrinsic error in velocity vector due to phase noise and residual motion errors is better than 4 cm/s, making motion due to waves the main source of error in the retrieved ATI currents. The paper points out that, if the DBI system were calibrated, it could supply some knowledge of wind conditions needed to remove these unwanted contributions.

Perkovic *et al.* (2004) and Perkovic *et al.* (2005), show results of DBI flights in low wind conditions (< 5 m/s) over the Gulf Stream western boundary with simultaneous measurements from a (nadir-pointing) IR radiometer. Data from a local NDBC weather buoy confirms that biogenic surfactant slicks seen in both IR and DBI images are aligned with the wind direction, except within the main jet of the Gulf Stream where they align with the underlying current. Uncorrected for wind and wave motions (thought to be small), the retrieved DBI currents give a realistic 2D current field consistent with the buoy wind data and the position and magnitude of the Gulf Stream jet.

3.10 Sletten (2006): An analysis of gradient-induced distortion in ATI-SAR imagery of surface currents

This paper investigates and quantifies the gradient-induced distortions of ATI surface velocity maps caused by the displacement in azimuth of moving targets that is typical of SAR imaging (the well-known “train-off-the-track” effect). As highlighted by Frasier & Camps (2001) and Siegmund *et al.* (2004), the problem is potentially serious for squinted dual-beam systems, where the displacement in azimuth differs in the fore and aft look, thus resulting in mis-registration of those pixels in the interferograms. A model is proposed to quantify the distortion of velocity gradients in azimuth, which can appear as compression or stretching of the true velocity profile. For velocity gradients beyond a critical threshold value defined as V/R (where V is the platform velocity and R is the range to the point on the surface), the distortion cannot be corrected.

The effect is particularly problematic to map currents in rivers, where strong gradients often occur. Over the ocean, a strong convergent oceanic front associated with high current gradient of the order of 10^{-2} s^{-1} ($\Delta u \sim 0.4 \text{ m/s}$ over 40 metres) will exceed the critical threshold for $R/V \geq 100$ (note the internal inconsistency with earlier statement), which is below that of spaceborne systems. Nevertheless, less than one resolution pixel would generally be affected by the distortion, although it may become visible under benign wind and wave conditions when the coherence time (and thus spatial resolution) is high enough.

3.11 Romeiser *et al.* (2010a): First Analysis of TerraSAR-X Along-Track InSAR-Derived Current Fields

This paper, which gives a fuller description of results first presented in Romeiser *et al.* (2009), shows the first examples of current retrieval from the spaceborne TerraSAR-X SAR system operated in ATI SAR mode. Contrary to SRTM, the only interferometric baseline for TerraSAR-X is along-track and is estimated to be around 0.8 metres. Interestingly, these are some of the first ATI data obtained at relatively small incidence angle (~ 30 deg).

The paper shows results of six passes obtained with TerraSAR-X in Aperture-Switching mode (AS) over the mouth of the River Elbe at various stages of the tide and for various



wind conditions. Various image averaging and processing are applied to remove spikes (from ships and permanent metal structures) and ghost echoes from land (linked to aliasing). Non-zero mean phase over land corresponding to horizontal velocities between -0.7 and 0.6 m/s is attributed to channel balancing applied to the raw data, and is removed using low-pass filtering over land extrapolated over water. Contributions by waves to the measured current are estimated with the model by Romeiser & Thompson (2000), to be up to 1 m/s based on local wind speed and direction data. However, the wave correction is found to be too large and is (arbitrarily) reduced by half in order to improve the comparison with currents from the UnTRIM numerical model (Figure 3).

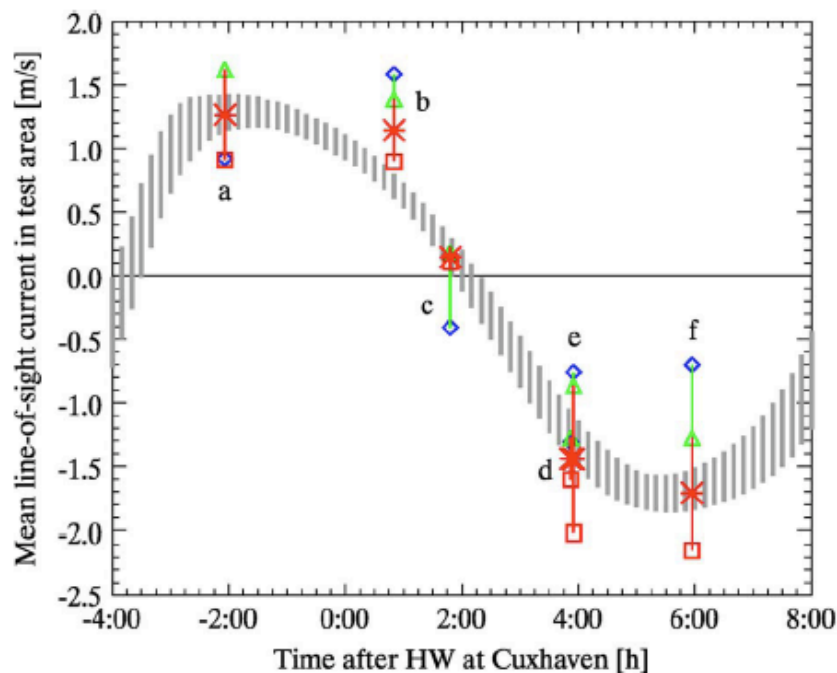


Figure 3: Temporal variations of spatial mean line-of-sight currents in River Elbe region as function of tidal phase, according to UnTRIM model and TerraSAR-X. Gray lines show range of UnTRIM current variations within the 32 tidal cycles available to us. Diamonds show uncorrected TerraSAR-X Doppler velocities for the six cases; triangles show Doppler velocities after phase recalibration based on apparent velocities over land. Lines between triangles and squares indicate theoretical maximum of further corrections for wave contributions according to our model, and asterisks show our best estimates of mean currents after applying 1/2 of these corrections (from Romeiser et al. (2010a))

In a similar vein, Suchandt *et al.* (2010), present TerraSAR-X ATI current measurements in the vicinity of Orkney Islands. It is stated that, with its 4.8 meters antenna, TerraSAR-X can operate in two ATI modes: Aperture Switching (where it alternately receives with the fore and aft part of the antenna) and Dual-Receive Antenna (where it receives simultaneously with both halves and separate electronics). Depending on the chosen configuration, the effective baseline takes values between 0.8 and 1.4 metres. Here, results are shown for AS mode with a baseline of around 1m. Realistic-looking current fields are retrieved in the energetic Pentland Firth strait (between Orkneys and north Scotland) although no validation data is presented.



Romeiser *et al.* (2010b), later present some of the few results obtained with TerraSAR-X operating in the more optimal dual-receive antenna (DRA) mode. The region corresponds again to the mouth of the Elbe River, using the same approach as used in Romeiser *et al.* (2010a). The authors point out the reduction in phase noise and smoother retrieved current fields in DRA than in AS mode, with current fields found to be consistent (after correction for wave contributions based on Romeiser & Thompson (2000)) with currents from the UnTRIM numerical model.

3.12 Kumagae *et al.* (2011): Sea Surface Current Measurement with Ku-Band SAR Along-Track Interferometry

This short IGARSS proceedings paper presents interesting results by a new group of investigators from Japan, from an ATI SAR current retrieval validation experiment near Cape Irago in Japan. The ATI SAR is an airborne system, which, unusually, operates at Ku-band and an incidence angle of 60 degrees. Two orthogonal flights at 10 minutes interval provide the two components of the currents. No information is provided on environmental conditions other than the average current velocity is 0.95 m/s. The SAR images are smoothed from a resolution of 0.6m to 35m to reduce the effect of phase noise. No further corrections are mentioned. The retrieved ATI SAR currents (0.82 m/s; northwest) compare well against data from a surface float equipped with a GPS logger (0.7-0.9 m/s; northwest).

3.13 Toporkov *et al.* (2011): Surface Velocity Profiles in a Vessel's Turbulent Wake Observed by a Dual-Beam Along-Track Interferometric SAR

This paper presents another example of airborne measurements obtained with the dual-beam interferometer (Frasier & Camps (2001); Toporkov *et al.* (2005)), this time with the aim of estimating the velocity of ships seen in the ATI images. The approach, previously also outlined in Toporkov *et al.* (2010), proposes to estimate ship velocity from the ATI images, as a way of calibrating ATI SAR phase in the open ocean when no land is visible in the ATI images. In this example however, the imaging of the ships is smeared due to motion effects, leading to an estimated uncertainty error around 0.2 m/s. While good information is available about wind and wave conditions, no attempts is made of retrieving ocean currents and no validation data is available to confirm the ship velocity or the observed velocity profiles across the ship wake.

3.14 Hansen *et al.* (2012): Simulation of radar backscatter and Doppler shifts of wave-current interaction in the presence of strong tidal current

While not strictly part of the literature relating to ATI SAR for ocean current retrieval, this paper presents an important recent development in our ability to model the microwave Doppler spectrum and its response to wind, waves and currents, particularly in the presence of strong wave-current interactions. The motivation for this work stems from growing interest in recent years in the retrieval of ocean currents from the shift of the Doppler spectrum centroid in conventional SAR images, as demonstrated by Chapron *et al.* (2005). The paper presents a new radar imaging model, DopRIM, which combines the Radar Imaging Model (RIM) by Kudryavtsev *et al.* (2005), with a Doppler shift estimation algorithm. The RIM model considers scattering contributions from specular reflections and



resonant (Bragg) scattering waves with local tilting effects due to longer underlying waves, as well as contributions by breaking waves in the form of specular reflections from very rough wave breaking zones based on the wave breaking statistics proposed by Phillips (1985). The Doppler shift predicted by the RIM model was shown by Johannessen *et al.* (2008) to compare well with Doppler shift observations from global Envisat ASAR Wide-Swath Medium resolution data in VV and HH polarisation and incidence angles of 23 and 33 deg. Further comparisons are presented of the modelled range Doppler velocities against Envisat ASAR estimates at VV and HH (Figure 4) and in the presence of strong tidal current in the Iroise Sea (off Brittany, France). Overall, although some discrepancies are revealed, the results suggest a dominant impact of strong surface currents and their modulation on both the radar-detected surface roughness and the range Doppler signals.

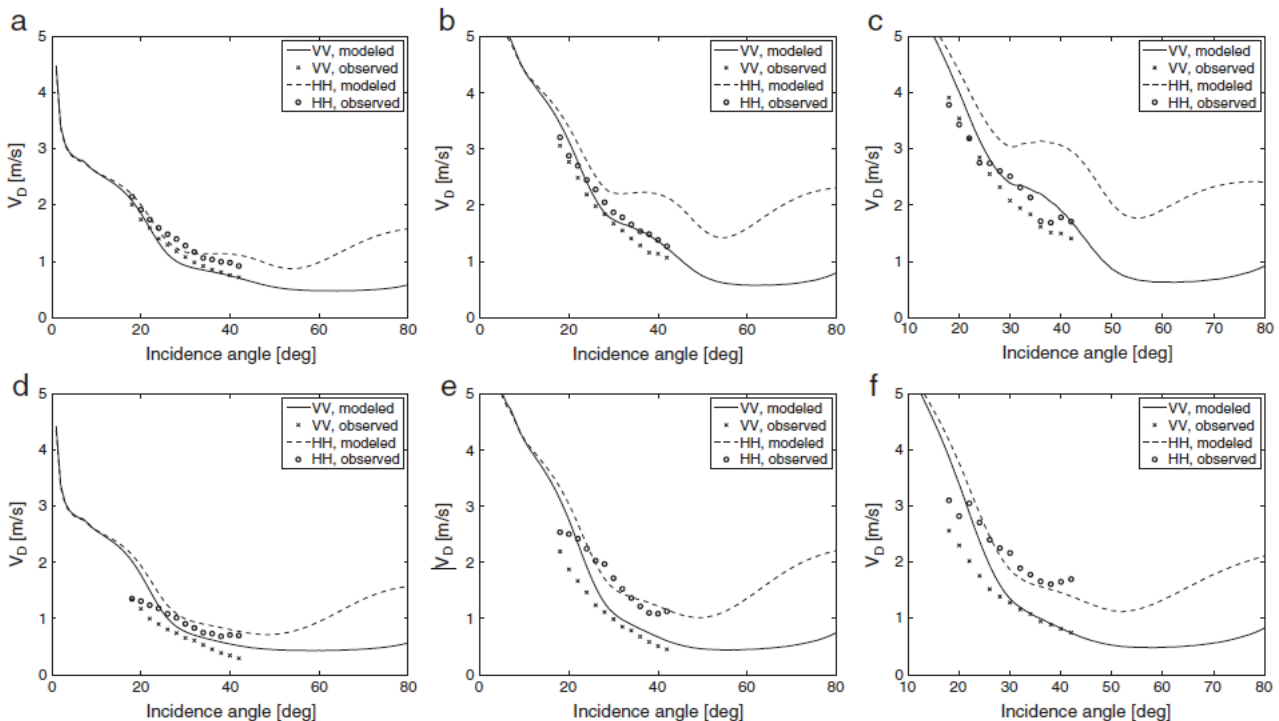


Figure 4: Range Doppler velocities for VV and HH polarization versus incidence angle at wind speed of 5 m/s (a and d), 10 m/s (b and e), and 15 m/s (c and f) in up- (a, b and c) and down-wind (d, e and f) configuration. 3% wind drift is included in V_D . The observations represent the median range Doppler velocities at the given wind conditions retrieved from nearly 2200 ASAR WSM acquisitions over the Norwegian Sea from August 2007 to February 2011 (about 1200 in VV and 1000 in HH polarization, respectively) (From: Hansen *et al.* (2012))



4 LITERATURE REVIEW SYNTHESIS

4.1 Interferometric SAR systems

The literature review revealed a wealth of past experimental studies focussed on ocean current retrieval with ATI SAR based on a wide range of interferometric SAR systems deployed from aircrafts (mainly), the space shuttle (SRTM) and from low-earth orbiting altitude (TerraSAR-X). Most radar systems featured along-track interferometric baseline only, although there is also some experience with systems featuring hybrid interferometric baselines, both from airborne platforms (Siegmond *et al.* (2004); Toporkov *et al.* (2005)) and from the higher altitude and platform velocity (233km; 7.5 km/s) of the Space Shuttle (Romeiser *et al.* (2005b)).

The literature survey suggests there has been a trend in radar frequency, migrating from early low frequency L-band ATI systems (e.g. Goldstein & Zebker (1987); Graber *et al.* (1996)) to recent systems operating at higher frequencies, such as X-band (e.g. Suchandt *et al.* (2010)) and Ku-band (Kumagae *et al.* (2011)). This evolution may be related to technological advances, and/or perhaps, is a response to modelling studies which predict better performance for ocean current retrieval at higher radar frequencies (Romeiser & Thompson (2000)).

Overall, with the exception of Siegmund *et al.* (2004), the chosen polarisation is VV, mainly for reasons of improved signal-to-noise ratio at far ranges in the swath. There is however a wide variety in the choice of incidence angles, several airborne systems choosing to span a wide incidence interval (20-70 deg; e.g. Goldstein & Zebker (1987); Anderson *et al.* (2003a)), while other focus on a narrow range of large to near-grazing incidences (60 deg in Kumagae *et al.* (2011); 70 deg in Toporkov *et al.* (2005)). In the only case of a system flown in low-earth orbit, TerraSAR-X opts (for reasons most probably unrelated to ATI concerns) for a narrow range of moderate incidence angles centred around ~30 deg.

So far, experience of current retrieval from interferometric SAR systems flown at higher altitudes has been gathered opportunistically from systems that were not primarily designed for along-track interferometry. Some authors repeatedly point out the limitations imposed by the hybrid across-track/along-track interferometric baseline of SRTM and by the limited azimuth sampling rate (PRF) and short effective along-track baseline of TerraSAR-X. For TerraSAR-X, these shortcomings are responsible for increased phase noise and ghost echoes of nearby land by aliasing, both of which have to be mitigated with the application of intensive averaging, smoothing and filtering (Romeiser *et al.* (2010a); Romeiser *et al.* (2010b); Suchandt *et al.* (2010)). For SRTM, the sensitivity of the phase to the height of surrounding land severely hinders the retrieval of sensible river flow values (Romeiser *et al.* (2007)). The problem is less critical over the flat landscape of the Dutch Wadden Sea (Romeiser *et al.* (2005b)) but the effect on current retrieval accuracy would need to be accounted for in any regions with marked water level changes across the scene. This crosstalk between height and current retrieval is well captured by the model proposed by Siegmund *et al.* (2004), which exposes the sensitivity of the hybrid interferometric phase to both elevation and velocity.



While squinted SAR systems are recognised as a major step forward in enabling both current vector components to be measured from a single pass, several authors point out the errors inherent to systems with hybrid baselines achieved with squinted beams. The retrieved velocity bias linked to the mis-registration in azimuth of moving surfaces in the fore and aft look of squinted systems is first highlighted by Frasier & Camps (2001), then by Siegmund *et al.* (2004). Later, Sletten (2006), gives a thorough analysis of the extent of the problem with a model that quantifies the distortion of ATI surface velocity maps, which depends on a threshold defined by V/R (with V is the platform velocity and R is the range to the point on the surface). The issue is deemed to be problematic for river flow estimation but not critical for oceanic features where typical current gradients will seldom be strong enough to result in major distortion of velocity fields seen by spaceborne systems. Another characteristic of squinted systems is the level of depolarisation of the signals, which will lead to a slight degradation of the SNR in single polarisation systems.

4.2 Experimental sites, environmental conditions and means of validation

The review of past experiments with ATI systems exposed a vast array of oceanographic settings. In most cases, the sites are characterised by strong tidal regime where maximum currents often reach in excess of 1 m/s. Only a few studies focussed on the detection of large-scale currents associated with mesoscale eddies and geostrophic jets (Anderson *et al.* (2003b; Goldstein & Zebker (1987); Perkovic *et al.* (2004)).

There is no example of anyone attempting to simultaneously measure height and currents over open ocean, the only example of joint retrieval being that of Siegmund *et al.* (2004), from a airborne hybrid interferometer flown over the estuary mouth of the Weser river.

Predominantly, experiment sites are located inshore, within sight of land. This may be because of limits of the aircraft range (in the case of airborne systems), or the availability of validation data (e.g. HF radar data in Graber *et al.* (1996) is constrained to 45km from land), or to ensure that land was imaged within the ATI scenes to provide the means to verify and calibrate the interferograms.

The means of validation of the ATI currents were, on the whole, disappointing. Far too often, validation consisted of comparisons with predictions from (more-or-less) operational numerical models, for which information is seldom given on the nature and quality of the forcing, or the performance of the model in predicting current speed and direction in the region of interest. Rare exceptions to this general rule are the exemplary validation set-up by Graber *et al.* (1996) (based on data from HF radar, weather buoys, directional wave buoys, current-meters and coincident ship campaigns) and validation against near-surface currents estimates using surface drifters (Goldstein *et al.* (1989; Kumagae *et al.* (2011)).

Information about wind conditions is usually given, although is typically provided by a weather station in the vicinity of (but not always within) the ATI scenes. Few papers consider how representative the in situ wind data may be of conditions across the wider scene. Perhaps because of the necessarily selective choice of papers considered in this review, only one study (Perkovic *et al.* (2004)) showed any attempt at deriving information on wind conditions from features within the ATI scenes in order to assist the interpretation of the ATI current data. Perhaps for the same reason, except for Graber *et al.* (1996;



Toporkov *et al.* (2011), information about wave conditions is inexistent, consisting at best of a passing comment on the visibility of long waves in the ATI scenes.

Overall, Graber *et al.* (1996), offers the only example where the experimental set-up provides the sufficiently complete characterisation of wind, wave, current and bathymetry conditions that is needed for a proper interpretation of observed ATI signatures.

4.3 Errors and mitigation strategies

4.3.1 ATTITUDE AND NAVIGATION ERRORS

There is an overwhelming consensus in the literature about the absolutely critical need to use accurate platform attitude and navigation data during processing to avoid unwanted fluctuations and biases in the phase and the resulting velocity fields. Even after correcting for attitude and navigation effects, low frequency fluctuations can remain (Toporkov *et al.* (2005); Romeiser *et al.* (2005b)) and contribute 0.1-0.2 m/s bias in velocity. Most studies mitigate these residual errors by calibrating the interferograms over land, setting the retrieved velocity over land to zero.

Aware that this mitigation strategy will not be applicable for ATI scenes in the open ocean where land is not imaged, Toporkov *et al.* (2011), explore the use of ships as targets of known velocity to calibrate the ATI phase. Unfortunately, the smearing of the ships in the SAR images (due to known issues about SAR imaging of moving targets) introduce an estimated uncertainty in the ship velocity of the order of 0.2 m/s, which makes this approach of limited use in its present form.

4.3.2 ERRORS SPECIFIC TO SQUINTED SYSTEMS

The reviewed papers that deal with squinted systems all highlighted two important additional issues inherent of squinted SAR.

4.3.2.1 DISTORSION BY STRONG CURRENT GRADIENTS

Frasier & Camps (2001), Siegmund *et al.* (2004) and Sletten (2006) all reported the issue of distortion induced by strong gradients, due to the mis-registration in azimuth of moving surfaces in the fore and aft look of squinted systems. Sletten (2006) quantifies the effect in relation to a threshold defined by V/R (with V is the platform velocity and R is the range to the point on the surface) and concludes that the effect is primarily problematic for river flow estimation but not critical for oceanic features observed with a spaceborne system. Nevertheless, this effect should be quantified for the Wavemill instrument configuration and orbits being considered for the mission.

4.3.2.2 POLARISATION MIXING

Another reported characteristic of squinted systems is the level of depolarisation of the signals, which leads to a slight degradation of the SNR in single polarisation systems. Ideally, the Wavemill system would operate in dual-polarisation on both transmit and receive to mitigate this problem. While this has severe implications for the design of the instrument and mission, it would bring considerable science benefits. Indeed, cross-polarised NRCS show less saturation at very high winds and provide the means to quantify contributions by breaking waves (Hwang *et al.* (2010)). Nevertheless, power levels in



cross-pol are several order of magnitude weaker than in co-polarised signals (see Figure 5), meaning that the instrument SNR would have to be improved considerably to achieve the necessary detection, especially at the edges of the swaths.

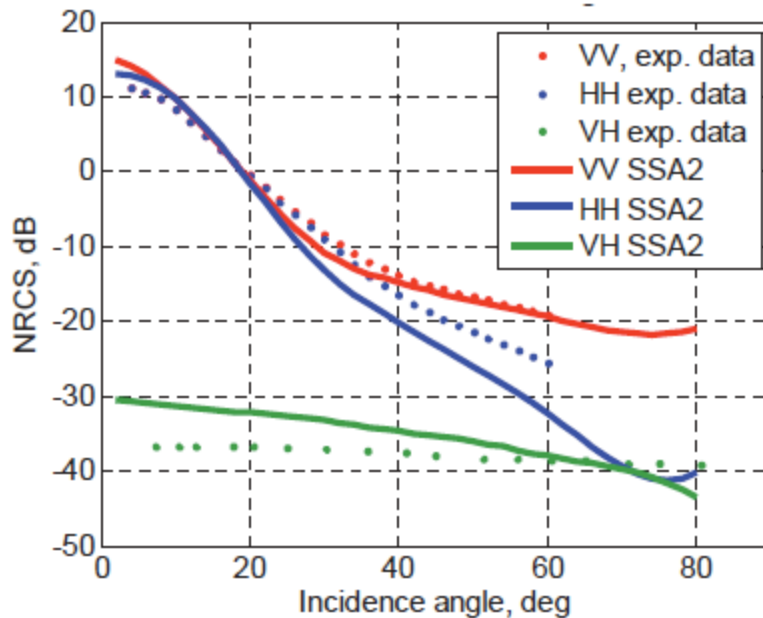


Figure 1. Measured (symbols) and calculated (curves) NRCS for all three polarization components as a function of incidence angle at X-band for 7.5 m/s wind speed (up-downwind).

4.3.3 FIGURE 5: MEASURED (SYMBOLS) AND SMALL-SLOPE APPROXIMATION OF THE 2ND ORDER CALCULATED (CURVES) NRCS FOR ALL THREE POLARISATION COMPONENTS AS A FUNCTION OF INCIDENCE ANGLE AT X-BAND FOR 7.5 M/S WIND SPEED, UP-DOWNWIND (FIGURE FROM VORONOVICH & ZAVOROTNY (2011); DATA FROM SKOLNIK (2008)) LONG SWELL WAVES

The contribution of long ocean swell waves to the ATI sensed surface displacement through the waves orbital motions is also widely acknowledged but not generally seen as a major issue. This long ocean swell wave effect is separate from, and an addition to, the ocean waves contribution to ATI sensed currents, which is usually removed via theoretical modelling (see more on this in next section). Typically, if swell waves are not visible in the high-resolution ATI images, swell correction is simply not applied, usually without appreciable detrimental effect on the quality of the current retrieval performance. Mostly, the effect of long swell waves is mitigated by degrading the spatial resolution of the retrieved current field to a resolution greater than the swell wavelength. This is achieved via averaging, smoothing and filtering of the high-resolution phase images, down to resolution of order 100 x 100 metres or even coarser (Goldstein *et al.* (1989; Romeiser *et al.* (2005b); Suchandt *et al.* (2010)). Of course, where fine spatial resolution wants to be retained (e.g. Toporkov *et al.* (2005)), there is presently no established strategy to mitigate the effect of swell on ATI currents.



4.3.4 WIND DRIFT

Similarly, the contribution to surface motion by wind drift is also recognised by several authors, and is typically estimated as 3 to 5 % of the wind speed at 10 metres in the direction of the wind. Here again, this contribution to surface displacement by wind is separate from, and in addition to, the unwanted surface motion related to the phase velocity of the (wind-generated) Bragg scatterers, which is usually removed via theoretical modelling (see more on this in next section). Unlike the orbital motions of long swell waves however, wind drift is a real displacement of water at the surface resulting from wind friction. It may be considered by some (e.g. those interested in ocean-atmosphere exchanges, or pollutant dispersal) as a legitimate constituent of the surface current that one wants to measure.

4.4 Theoretical modelling and model performance

It is generally agreed that, apart from the errors mentioned in the previous section, unwanted contributions by ocean surface waves (other than long ocean swell which are dealt with separately) are the most important cause of errors in ATI retrieved currents.

The phase velocity of the Bragg scatterers (responsible for the backscatter) can, by itself, account for up to 0.5 m/s of the observed discrepancy with validation data. The exact contribution by Bragg scatterers is, in fact, highly dependent on having good knowledge of wind direction and on the assumed wave spectrum directional spreading function.

The surface wave contribution is usually quantified and removed using a theoretical scattering model. Several models have been developed and used in the papers surveyed in this review.

Graber *et al.* (1996), successfully estimated and removed unwanted wave motions by using the theoretical model described by Thompson *et al.* (1991). This model, based on the computationally expensive time-dependent model by Thompson (1989), has the merit of having been validated against measured Doppler spectra obtained at L-band and Ku-band (Figure 6). Graber *et al.* (1996), also benefited from excellent in situ measurements of wind and wave spectra, which were used as input to the scattering model.

Romeiser & Thompson (2000), proposed a new more efficient model to compute the Doppler spectrum, and this theoretical model has been used extensively to correct for wave-induced motion, with more or less success (Anderson *et al.* (2003a; Romeiser *et al.* (2005b; Romeiser *et al.* (2010a; Romeiser *et al.* (2010b; Siegmund *et al.* (2004)). One limitation of the model is that it relies on the weak hydrodynamic modulation of wave spectrum by currents according to Romeiser & Alpers (1997), which may not hold in presence of strong currents. Unlike Thompson *et al.* (1991), the authors presented no evidence of validation of the Doppler shift against observations. In comparisons of retrieved ATI velocities against independent current estimates, this model was found to overestimate the contribution by surface waves Romeiser *et al.* (2010a), and was (arbitrarily) reduced by half to improve the agreement with the validation data.

Finally, Hansen *et al.* (2012) presents recent developments in theoretical modelling of microwave scattering, used for current retrieval from Doppler centroid shift in conventional



SAR systems (e.g. Envisat ASAR). In addition to the scattering contributions contained in Romeiser & Thompson (2000), the new DopRIM model also accounts for scattering by specular reflections and wave breaking, which are important at low incidence angle (~ 20 - 30 deg) and in the presence of strong current gradients. The backscatter and shift of the Doppler spectrum centroid predicted by the model shows better polarisation ratio than models based solely on composite two-scale scattering, and benefits from having been extensively validated against observations from Envisat ASAR, including in conditions of strong currents.

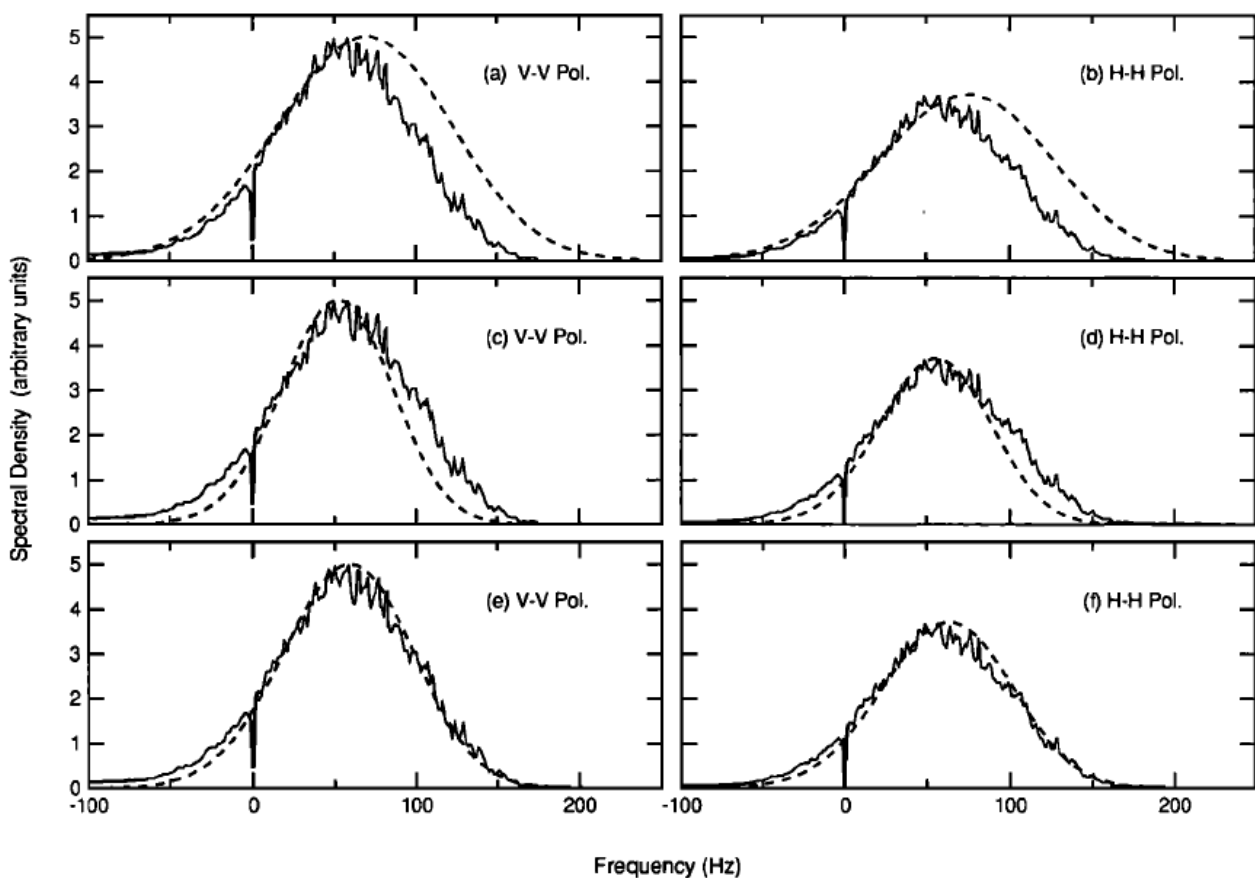


Figure 6: Comparison of measured Doppler spectra with predictions using (a,b) an empirical wave number spectrum, (c,d) the augmented wire gauge spectrum, and (e,f) the augmented pressure sensor array spectrum. Data and predictions obtained for Ku-band and incidence angle of 20 degrees (From: Thompson et al. (1991))



5 IMPLICATIONS FOR A FUTURE SPACEBORNE WAVEMILL MISSION

The analysis of the literature has brought to light a number of points, which will need to be considered as part of the design of a spaceborne Wavemill mission.

These consist of:

- 1) the need to ensure the availability of precise attitude and navigation data at high rate and their use during processing of the interferograms. Unfortunately, the required level of accuracy and update rate cannot be precisely determined from the literature review, since insufficient details are given in the reviewed papers about the sensitivity of the retrieved current (or measured phase) to platform attitude and height error. Further dedicated activities will be needed to properly quantify these requirements in terms of their impact on current retrieval performance.
- 2) the need for a strategy to calibrate the interferometric phase to remove residual attitude and navigation errors. Even after correction, all investigators report residual variations in phase, which can translate into large fluctuations in retrieved currents. For example, Romeiser *et al.* (2005a) reports that antenna oscillations measured onboard SRTM with accuracy of 3mm, still resulted, after compensation, to residual “motion” errors with phase variations of the order of 0.1 rad, equivalent to horizontal velocity of 0.6 m/s. Issues to consider are how frequently the phase should be calibrated, whether the calibration strategy has to rely on imaging of land in all scenes (which would limit ATI acquisitions to within 100 km or so of land) or if the phase over ocean-only scenes can be calibrated using other means.
- 3) the need to optimise radar parameters to avoid aliasing . This includes choosing an effective along-track baseline, but also a careful choice of PRF to ensure adequate azimuth sampling and thus avoid aliasing, which produces ghost echoes of land over water that are difficult to remove (see Romeiser *et al.*, 2010a; Suchandt *et al.*, 2010)
- 4) the need to quantify the impact on current retrieval performance of the choice of squint angle, incidence angles and platform altitude/velocity, given:
 - a) biases in current retrieval due to azimuth mis-registration in squinted beams;
 - b) reduced signal to noise ratio due to polarisation mixing, and thus with secondary implications for the power and mass budget, swath width, coverage, revisit time and mission lifetime.

Dual-polarisation would mitigate the latter to some extent, and is also scientifically highly desirable by providing useful information about wind and wave breaking effects. However, full dual-pol capability would strongly impact the design of the instrument and the mission. Dual-polarisation on receive channels only may offer a useful compromise, but only if high-enough SNR can be achieved.



6 IMPLICATIONS FOR WAVEMILL OCEAN CURRENT PRODUCTS

The literature review highlighted several outstanding scientific issues, some of which have implications for the Wavemill scientific products.

- 1) With ocean penetration depths at Ku-band typically less than 1 mm, Wavemill will sense all phenomena that impart velocity to the top layer of the ocean surface. These include:
 - a) unwanted velocities that are sensed by radars but do not contribute to water mass transport i.e. the phase velocity of the Bragg waves and the orbital motion of longer ocean waves. Their impact can be quantified and removed if wind and wave conditions are known.
 - b) All currents affecting the surface, including wind-induced currents (Ekman), Stokes drift, tidal currents, geostrophic currents, surface divergence and convergence flows, Langmuir circulation,...

These current components all vary on different temporal and horizontal scales, as well as with depth, making it a challenge to validation (see below). Wavemill will measure the “total current”, consisting of the sum of these various components as they are expressed at the air-sea interface. Separation into individual components is desirable and may be possible for some components, but would need to be clearly identified and defined in the Wavemill products.

- 2) Separating wind, wave and current contributions in the measured interferometric phase remains an important issue and a serious challenge. Wave breaking is known to play an important role, so any wind/wave mitigation strategy should ideally use one of the recent scattering models, which seek to account for wave breaking. With the relative importance of wind, waves and current effects changing also with radar frequency, polarisation and incidence angle, more extensive use should be made of present-day knowledge of microwave scattering from latest theoretical advances and recent experiences with Envisat ASAR, Radarsat-2 and TerraSAR-X when defining the Wavemill instrument and mission.
- 3) Validating Wavemill surface currents will present unprecedented difficulties, insofar as traditional sources of data used for validation of currents may not be appropriate to validate currents measured by Wavemill. Arguably, HF radars offer the closest match to Wavemill surface currents, although their much lower radar frequency will make them sensitive to currents as perceived by long ocean waves (25 meters or longer, depending on the HF radar frequency). Other means of validation, like current-meters and Acoustic Doppler Current Profilers (ADCP), will accurately measure currents at a given depth, but seldom report data closer than a few meters from the surface, thereby overlooking the strong vertical current shear in the top few meters. Finally, surface drifters could offer an acceptable solution, depending on drifter size and the depth of their drogue. All things considered, the simple flat plywood drifters developed and deployed by Goldstein *et al.* (1989) to validate airborne ATI currents may yet offer the best solution to measure truly near-surface water displacement, while minimizing the influence of wind drag on the body of the drifter.



7 CONCLUSIONS

We presented the results of an in-depth review of the literature on the retrieval of ocean currents with ATI SAR systems.

The analysis covered a broad range of experimental and theoretical studies, and focussed on reviewing existing experience on the following aspects:

- basic parameters of past interferometric SAR systems
- experiments with ATI for current retrieval, documenting environmental conditions and the means of current validation used
- reported errors and proposed mitigation strategies
- Theoretical models to mitigate surface wave effects and their performance against observations

The main implications for the development of the Wavemill instrument and mission are:

- There remains a need to perform end-to-end performance assessments of Wavemill to precisely quantify the requirements on attitude and navigation information needed to achieve the desired current retrieval accuracy.
- A phase validation strategy should be devised to independently assess residual phase errors after removal of platform-related errors. Even with state-of-the-art attitude and navigation data, residual errors will remain and will need to be quantified for removal prior to geophysical inversion.
- Full dual-polarisation capability is scientifically highly desirable and would help mitigate to some extent the SNR reduction associated with polarisation mixing in squinted systems. Partial dual-pol (i.e. on receive channels only) would offer a useful compromise, but only if high-enough SNR can be achieved.

The main implications for the definition of the Wavemill products are:

- By nature, Wavemill currents will differ considerably from currents measured by traditional means, making validation difficult. Some separation of the “total” current measured by Wavemill into individual current components is desirable (e.g. for validation and exploitation) and may be achievable in some cases. In all cases, currents components provided in the Wavemill products should be unambiguously identified and clearly defined.
- Separating wind, wave and currents contributions remains challenging, and could seriously spoil the perceived accuracy and usefulness of Wavemill current data. Better use could be made of recent advances in microwave scattering models to define a Wavemill instrument and mission for which these inversion problems are more tractable.



ANNEX A: SUMMARY TABLE FOR KEY PUBLICATIONS RELEVANT TO ATI SAR OCEAN CURRENTS

Reference	Radar system & geometry	Spatial Resolution	What & where	Environmental conditions & retrieval accuracy	Validation data sources	Errors, mitigation strategies & modelling
Goldstein & Zebker (1987)	Airborne, L-band Alt: 8km; V: 238 m/s Two antennas; TRR B _{AT} : 18.5 m I: 20-57 deg	12(AT) x 11(XT) m Smoothed to 60x60m for currents E-W component only	Currents San Francisco Bay, USA	+ 30 minutes from maximum tidal flow (2.6 m/s) Currents: eddies (small: 1.6 m/s; large: 0.8 m/s) Wind: "relatively smooth surface" Waves: "little swell" Accuracy: 0.04 m/s @ 60 x 60 m	Tidal current tables	Yawing error => corrugations in XT direction Yaw error of 0.01 deg = current error of 4 cm/s
Goldstein et al. (1989)		Phase averaged to 100 x 100 metres	Currents San Diego, Mission Bay, Point Loma, USA	Maximum tidal flow Wind: < 6 m/s, SW Waves: "extensive", including diffraction, contributing up to 1.5 m/s to line-of-sight velocity	Surface drifters made of plywood 1.2m x 0.6m x 2cm deep, positioned by Loran-C	Biases in phase due to yaw error and navigation uncertainty Swell mitigated by averaging to 100x100m Bragg contribution estimated over calm water (0.5 m/s) compares well with theoretical estimates
Marom et al. (1990)			Wave spectra Monterey Bay, USA	Bimodal waves travelling close to radar line-of-sight (favourable) Wind: Light (< 2m/s) Waves: low (< 0.6m)	Wave pressure sensor	



Graber <i>et al.</i> (1996)	Airborne, L-band V: 200m/s Two antennas, TRR B _{AT} : 20m Lag time: 0.05s (decorrelation @ L-band: 0.3-0.4s in light-moderate winds I: 20-60 deg	10(AT) x 10(XT) m Two components (orthogonal flights)	Currents Cape Hatteras, along inshore edge of Gulf Stream north wall, USA	Four flight passes on 20 June 1993 Wind: 5-6 m/s; 235 deg	HF radar (1km resolution out to 45km offshore) Two research ships (ADCP currents & density profiles) Two buoys for meteo, directional wave & currents at 10-meters	No GPS system during flights to correct navigation and attitude effects => uses flat motionless target (Outer Banks) to calibrate phase Two techniques to mitigate surface wave motion effects: - microwave scattering model by Thompson, 1989, and Thompson <i>et al.</i> (1991), with some knowledge of local wind and wave field - calibration with in situ current data at different range locations in image
Romeiser & Thompson (2000)	N/A	N/A	Currents Numerical simulations only	N/A	N/A	New efficient model to compute Doppler spectra, assuming weak hydrodynamic modulation of ocean surface wave spectra according to Romeiser & Alpers (1997)
Frasier & Camps (2001)	N/A	N/A	Currents Instrument design	N/A	N/A	Design for squinted ATI-SAR system, with formulation of the response including effects of attitude and velocity errors, polarisation mixing and phase biases due to azimuthal displacement of moving surfaces.
Frasier <i>et al.</i> (2001)	Airborne, C-band VV pol Squinted B _{AT} : 1 m	N/A	Currents	N/A	N/A	Instrument prototype of design above



Junek et al. (2003)	Alt: 600 m, V: 100 m/s I: 69-86 deg Squint: 20 deg	Swath ~ 7km 16.7 (XT) m	Charlotte Harbour, Florida, USA	Biogenic surfactant slicks (i.e. wind < 5 m/s)		First airborne trials of prototype above Different backscatter intensity in forward and aft looks, attributed to directionality of surface wave spectrum (Bragg)
Anderson et al. (2003a)	Airborne, L & C-band JPL AIRSAR Alt: 8.6km, V: 216m/s B _{AT} : 19m (L) B _{AT} : 1.9m (C) I: 23-73 deg	10(AT) x 6(XT) m	Currents and waves Hawaii (close to north tip of Big Island), USA	Current: 0.25m/s (tide) Wind: strong wind shear (orographic effects) Waves: swell present	None	Un-calibrated amplitude and phase Strong phase gradients due to poor aircraft attitude control Modelling: ATI phase modelled with composite model by Romeiser & Thompson (2000) with input from OCCAM & HOME tidal currents coupled with WAM 3rd generation wave model (wave-current interactions) and ECMWF winds
			Kuroshio, SW Japan	Current: Kuroshio jet and eddy (1m/s)	None	
Siegmund et al. (2004)	Airborne, X-band Hybrid AT/XT (squinted) HH pol Alt: 3.2km, V~80m/s B _{AT} : 0.034m B _{XT} : 1.56m I: 45 deg	0.5(AT) x 0.5(XT) m Accuracy: 0.2m/s	Land elevation and currents Estuary mouth of Weser river, Wadden Sea, German Bight	Shallow inter-tidal zone; tidal range: 3.6m Current: + 30 minutes from low tide; Max current: 0.7-0.9m/s Wind: 8-10m/s	Hydrodynamic model (TRIM-2D) Coastal weather station	Model to quantify ambiguity between elevation and velocity retrieval in hybrid Interferometric phase Mis-registration in azimuth due to XT baseline leads to bias in phase because of squint. Remove wind drift (3% Wind speed) and Bragg waves phase velocity (~0.2m/s) estimated with Romeiser & Thompson (2000) Resolves elevation from currents with two anti-parallel flights 10min apart.



<p>Romeiser et al. (2005b)</p>	<p>SRTM, X-band Hybrid AT/XT VV pol Alt: 233km, V: 7500m/s B_{AT}: 7 m (effective: 3.5m) B_{XT}: 60m I: 55 deg Phase sensitivity: 10 deg per m/s</p>	<p>Amplitude averaged to 200x200m Phase averaged to 100x100m Accuracy ~ 0.24 m/s rms at 1 km</p>	<p>Currents Dutch Wadden Sea, The Netherlands</p>	<p>-3h from high water Current: strong tidal flow (1.2 m/s) Wind: 5m/s westerly (coastal met stations)</p>	<p>Hydrodynamic model (KUSTWAD with old bathymetry) Correlation > 0.5 for scales > 1km</p>	<p>Un-calibrated phase => set velocity to 0 close to land High-pass filtering to remove phase variations 20km and longer. 100x100m phase smoothed with 5x5 pixel running boxcar filter, 3 times Wave contributions modelled with Romeiser & Thompson (2000), using KUSTWAD currents and in situ wind. Wave-current interactions and non-linear effects neglected, surface wave spectrum adjusted to be in equilibrium with local effective wind (wind vector minus local current vector) Differences between ATI modelled and KUSTWAD currents mainly at scales > 10km, assigned to residual errors due to SRTM mast oscillations.</p>
<p>Romeiser et al. (2007)</p>	<p>Same as above</p>	<p>Amplitude & phase averaged to 100x100m</p>	<p>Currents Elbe River, Germany</p>	<p>-1h from low water Wind: 5m/s, WNW Wind against current</p>	<p>None</p>	<p>Meandering river shows phase varies depending on orientation of the river with respect to radar look direction Smoothing & processing as above Phase calibrated by assuming constant current velocity over 90deg river meander No correction for wave contribution (model not adapted for rivers)</p>



Toporkov et al. (2005)	Airborne, C-band VV pol Alt: 600m, V: 100m/s Four squinted antennas (± 20 deg from broadside) Only fore antenna transmit $B_{AT} = 1.23m$ (effective: 0.6m) I: 70 deg (60-82 in squinted plane)	Range within swath: 1.2-4.4 km 0.6m(AT) x 6m(XT), multi-looked in azimuth ("coarse-graining") to 6m x 6m	Currents Inlets of Florida Barrier islands (Captiva Pass, Redfish Pass)	Maximum ebb flow Wind: 3-5 m/s, E or 5-6 m/s, NE Waves: none visible in 6 x 6m resolution images	Daily current predictions from NOAA National Ocean Service One aerial photograph (from ~ 1 year earlier)	GPS/DGPS for attitude/position at 10Hz for motion compensation during SAR processing Phase averaged to 120m x 120m for velocity retrieval in regions of low coherence (noisy phase) No correction for surface wave motion but wave contribution estimated to be up to 0.5 m/s Uncorrected phase undulations in azimuth (0.1 rad) are estimated to yield bias in velocity vector of 0.17 m/s, which matches well with non-zero velocity observed over land.
Toporkov et al. (2004)	Same as above	Same as above	Same as above	Same as above	Same as above	Same as above
Perkovic et al. (2004)	Same as above	Same as above	Gulf Stream western boundary, east of Cape Canaveral	Wind: 4.9 m/s, SE	NDBC weather buoy (41009)	Simultaneous measurements with DBI and IR radiometer over Gulf Stream western boundary Biogenic surfactant slicks in IR and DBI aligned with wind direction, except within Gulf Stream jet
Perkovic et al. (2005)	Same as above	Same as above	Florida Barrier islands & Gulf Stream	Same as above	Same as above	Same as above



<p>Romeiser et al. (2010a)</p>	<p>TerraSAR-X X-band, VV pol Alt: 514 km Aperture-switching mode B_{AT}: 0.8m (effective) I: 31.0 - 32.5 deg Phase sensitivity: 1.3 deg per m/s</p>	<p>Swath: 16 km 0.92 (AT) x 2.12 (XT) m Phase averaged to 100x100m</p>	<p>Currents Mouth of Elbe River, Germany</p>	<p>Six passes between 7 May and 23 July 2008 -2 to +5 hours from high water Wind: 3.3 to 7.2 m/s</p>	<p>Permanent gauging stations High-resolution (100m, 10min) 3D current fields from numerical UnTRIM model (2006 run)</p>	<p>Remove contributions from ships and permanent metal structures Filtering to remove ghost echoes from land Non-zero mean phase over land equivalent to velocity -0.7 to +0.6 m/s are attributed to channel balancing applied to raw data => low-pass filtering over land extrapolated over water Wave contributions removed with Romeiser & Thompson (2000) model (up to 1m/s) Wave correction too large => only apply ½ correction (arbitrarily)</p>
<p>Romeiser et al. (2010b)</p>	<p>TerraSAR-X Dual-receive antenna mode B_{AT}: 1.1m (effective)</p>	<p>Full-resolution interferogram pixel spacing: 1 m²</p>	<p>Currents Mouth of Elbe River, Germany</p>	<p>Two passes in Spring 2009 No environmental information</p>	<p>Same as above</p>	<p>Wave contributions (up to 1m/s) removed with Romeiser & Thompson (2000) Smoother current fields in DRA, consistent with UnTRIM model</p>



<p>Suchandt et al. (2010)</p>	<p>TerraSAR-X Aperture-switching mode B_{AT}: 1.02m I: 31.4 deg Phase sensitivity: 0.03 rad (1.7 deg) per m/s</p>	<p>Swath: 100 x 5km Averaged 100x100m to</p>	<p>Currents Orkney Islands and Pentland Firth, UK</p>	<p>N/A</p>	<p>None</p>	<p>Spike removal procedure (ships) Resulting velocity field smoothed with 5x5 pixel running boxcar filter, 3 times Limited azimuth sampling causes azimuth ambiguities, visible as “ghost images”, originating from the side lobes of the azimuth antenna diagrams wrapped into the base band. Need to apply a Doppler filter to let pass the motion signal and stop the ambiguity parts. Phase over land set to zero Doppler velocities corrected for mean contributions of wave motions using same procedure as Romeiser et al. (2010a). Wave contributions = 1.1m/s (wind speed = 8m/s @ 10deg from radar look direction), -0.69m/s (W = 4m/s @ 150deg) and 0.63 m/s (W = 4m/s @ 35 deg).</p>
<p>Kumagae et al., 2011</p>	<p>Airborne, Ku-band VV pol B_{AT}: 0.2m I: 60 deg</p>	<p>Two components (orthogonal flights) ATxXT: 0.6m Averaged 35x35m to</p>	<p>Currents Cape Irago, Japan</p>	<p>N/A</p>	<p>Surface float with GPS logger ATI current: 0.82m/s, NW Float current: 0.7-0.9 m/s, NW</p>	<p>Velocity set to zero over static targets</p>



Toporkov et al. (2011)	Same as Toporkov et al. (2005)	6m x 6m	Ship velocity 80 km southwest of Tampa, Florida	Wind: (coastal station) 4m/s, ESE; (NDBC buoy 42036) 7.5 m/s, ESE Waves: (NDBC buoy 42036) Dominant Wave Dir: 158 deg; Significant Wave Height: 1.24m; Dominant wave period: 6.25s	None	Attempts to estimate ship velocity as a possible way of calibrating ATI phase away from land. Ship image is smeared due to motion effects, leading to 0.2 m/s estimated uncertainty in ship velocity
Hansen et al. (2012)	N/A	N/A	Currents from conventional SAR (Doppler centroid shift)	N/A	N/A	New theoretical scattering model to compute microwave backscatter and Doppler shift accounting for composite Bragg scattering, specular reflections and contributions by breaking waves. Presents validation of Doppler velocity against observations from Envisat ASAR in Norwegian Sea and in Iroise Sea in presence of strong current gradients.

Key: AT: Along-track; XT: across-track (or range); Alt: platform altitude; B: antenna baseline; I: incidence angles (0 deg = nadir); TRR: ATI mode where fore antenna transmits and both fore/aft receive;



8 LIST OF ACRONYMS

BNSC	British National Space Centre
SAR	Synthetic Aperture Radar
SRTM	Shuttle Radar Topography Mission
SWH	Significant Wave Height (aka H_s or “wave height”)
TN	Technical Note
WP	Work Package



9 BIBLIOGRAPHY

Anderson, C., T. Macklin, C. Gommenginger, M. Srokosz, J. Wolf, D. J. T. Carter, E. Ash, A. Thornbury, and C. D. Hall, 2003a, Along Track SAR Interferometry for Ocean Currents and Swell. Final report of the British National Space Centre NEWTON Contract CU009-017539, 40 pp

Anderson, C., T. Macklin, J. Wolf, C. Gommenginger, and M. Srokosz, 2003b: Observations and modelling of the response of along-track SAR interferometry to mesoscale ocean features. *Igarss 2003: IEEE International Geoscience and Remote Sensing Symposium, Vols I - VII, Proceedings*, 1927-1929.

Chapron, B., F. Collard, and F. Ardhuin, 2005: Direct measurements of ocean surface velocity from space: Interpretation and validation. *Journal of Geophysical Research-Oceans*, 110.

Farquharson, G., W. N. Juneak, A. Ramanathan, S. J. Frasier, R. Tessier, D. J. McLaughlin, M. A. Sletten, and J. V. Toporkov, 2004: A Pod-Based Dual-Beam SAR. *IEEE Geoscience and Remote Sensing Letters*, 1, 62-65.

Frasier, S. J., J. R. Carswell, and J. Capdevila, 2001: A pod-based dual-beam interferometric radar for ocean surface current vector mapping. *Igarss 2001: Scanning the Present and Resolving the Future, Vols 1-7, Proceedings*, 561-563.

Frasier, S. J., and A. J. Camps, 2001: Dual-beam interferometry for ocean surface current vector mapping. *IEEE Transactions on Geoscience and Remote Sensing*, 39, 401-414.

Goldstein, R. M., and H. A. Zebker, 1987: Interferometric Radar Measurement of Ocean Surface Currents. *Nature*, 328, 707-709.

Goldstein, R. M., T. P. Barnett, and H. A. Zebker, 1989: Remote-Sensing of Ocean Currents. *Science*, 246, 1282-1285.

Graber, H. C., D. R. Thompson, and R. E. Carande, 1996: Ocean surface features and currents measured with synthetic aperture radar interferometry and HF radar. *Journal of Geophysical Research-Oceans*, 101, 25813-25832.

Hansen, M. W., V. Kudryavtsev, B. Chapron, J. A. Johannessen, F. Collard, K. F. Dagestad, and A. A. Mouche, 2012: Simulation of radar backscatter and Doppler shifts of wave-current interaction in the presence of strong tidal current. *Remote Sensing of Environment*, 120, 113-122.

Hwang, P. A., B. A. Zhang, J. V. Toporkov, and W. Perrie, 2010: Comparison of composite Bragg theory and quad-polarization radar backscatter from RADARSAT-2: With applications to wave breaking and high wind retrieval. *Journal of Geophysical Research-Oceans*, 115.



Johannessen, J. A., B. Chapron, F. Collard, V. Kudryavtsev, A. Mouche, D. Akimov, and K. F. Dagestad, 2008: Direct ocean surface velocity measurements from space: Improved quantitative interpretation of Envisat ASAR observations. *Geophysical Research Letters*, 35.

Junek, W. N., A. Ramanathan, G. Farquharson, S. J. Frasier, R. Tessier, D. J. McLaughlin, M. A. Sletten, and J. V. Toporkov, 2003: First observations with the UMass dual-beam InSAR. *Igarss 2003: IEEE International Geoscience and Remote Sensing Symposium, Vols I - VII, Proceedings*, 530-532.

KoRIOLiS, 2002: Study on Concepts for Radar Interferometry from satellites for Ocean (and Land) Applications(KoRIOLiS). Final report. Available from <http://www.ifm.uni-hamburg.de/~romeiser/koriolis.htm>.

Kudryavtsev, V., D. Akimov, J. Johannessen, and B. Chapron, 2005: On radar imaging of current features: 1. Model and comparison with observations. *Journal of Geophysical Research-Oceans*, 110.

Kumagae, N., K. Kawamura, K. Tatsumi, M. Furuhashi, M. Tsuchida, M. Tsuji, T. Yamaoka, and K. Suwa, 2011: Sea Surface Current Measurement with Ku-Band Sar Along-Track Interferometry. *2011 IEEE International Geoscience and Remote Sensing Symposium (Igarss)*, 1465-1468.

Marom, M., R. M. Goldstein, E. B. Thornton, and L. Shemer, 1990: Remote-Sensing of Ocean Wave Spectra by Interferometric Synthetic Aperture Radar. *Nature*, 345, 793-795.

Perkovic, D., J. V. Toporkov, M. A. Sletten, G. Farquharson, S. J. Frasier, G. O. Marmorino, and K. P. Judd, 2004: Gulf Stream observations obtained with the UMass dual beam interferometer and an infrared camera. *Igarss 2004: IEEE International Geoscience and Remote Sensing Symposium Proceedings, Vols 1-7*, 3325-3328.

Perkovic, D., S. J. Frasier, R. Tessier, M. A. Sletten, and J. V. Toporkov, 2005: An airborne pod-mounted dual beam interferometer. *2005 IEEE Aerospace Conference, Vols 1-4*, 1193-1201.

Phillips, O. M., 1985: Spectral and Statistical Properties of the Equilibrium Range in Wind-Generated Gravity-Waves. *Journal of Fluid Mechanics*, 156, 505-531.

Romeiser, R., and W. Alpers, 1997: An improved composite surface model for the radar backscattering cross section of the ocean surface—Part II: Model response to surface roughness variations and the radar imaging of underwater bottom topography. *Journal of Geophysical Research*, 102, 251–225 267.

Romeiser, R., and D. R. Thompson, 2000: Numerical study on the along-track interferometric radar imaging mechanism of oceanic surface currents. *IEEE Transactions on Geoscience and Remote Sensing*, 38, 446-458.



- Romeiser, R., J. Sprenger, D. Stammer, H. Runge, and S. Suchandt, 2005a: Global current measurements in rivers by spaceborne along-track InSAR. *IGARSS 2005: IEEE International Geoscience and Remote Sensing Symposium, Vols 1-8, Proceedings*, 71-74.
- Romeiser, R., H. Breit, M. Eineder, H. Runge, P. Flament, K. de Jong, and J. Vogelzang, 2005b: Current measurements by SAR along-track interferometry from a space shuttle. *Ieee Transactions on Geoscience and Remote Sensing*, 43, 2315-2324.
- Romeiser, R., H. Runge, S. Suchandt, J. Sprenger, H. Weilbeer, A. Sohrmann, and D. Stammer, 2007: Current measurements in rivers by spaceborne along-track InSAR. *Ieee Transactions on Geoscience and Remote Sensing*, 45, 4019-4031.
- Romeiser, R., S. Suchandt, H. Runge, and U. Steinbrecher, 2009: Analysis of First Terrasar-X Along-Track Insar-Derived Surface Current Fields. *2009 Ieee International Geoscience and Remote Sensing Symposium, Vols 1-5*, 272-275.
- Romeiser, R., S. Suchandt, H. Runge, U. Steinbrecher, and S. Grunler, 2010a First Analysis of TerraSAR-X Along-Track InSAR-Derived Current Fields. *Ieee Transactions on Geoscience and Remote Sensing*, 820-829.
- Romeiser, R., S. Suchandt, H. Runge, and H. Graber, 2010b, Currents in Rivers, Coastal Areas, and the Open Ocean from Terrasar-X Along-Track Insar. *2010 Ieee International Geoscience and Remote Sensing Symposium*, 3059-3062.
- Siegmund, R., M. Q. Bao, S. Lehner, and R. Mayerle, 2004: First demonstration of surface currents imaged by hybrid along- and cross-track interferometric SAR. *Ieee Transactions on Geoscience and Remote Sensing*, 42, 511-519.
- Skolnik, M., 2008: *Radar Handbook, 3rd edn.* McGraw-Hill.
- Sletten, M. A., 2006: An analysis of gradient-induced distortion in ATI-SAR imagery of surface currents. *Ieee Transactions on Geoscience and Remote Sensing*, 44, 1995-2002.
- Suchandt, S., H. Runge, R. Romeiser, N. Tous-Ramon, and U. Steinbrecher, 2010: Tidal Current Measurement with Terrasar-X Along-Track Interferometry. *2010 Ieee International Geoscience and Remote Sensing Symposium*, 2432-2435.
- Thompson, D. R., 1989: Calculation of Microwave Doppler Spectra from the Ocean Surface with a Time-Dependent Composite Model. *Radar Scattering from Modulated Wind Waves*, G. J. Komen, and W. A. Oost, Eds., Springer Netherlands, 27-40.
- Thompson, D. R., B. L. Gotwols, and W. C. Keller, 1991: A Comparison of Ku-Band Doppler Measurements at 20-Degrees Incidence with Predictions from a Time-Dependent Scattering Model. *Journal of Geophysical Research-Oceans*, 96, 4947-4955.
- Toporkov, J. V., M. A. Sletten, D. Perkovic, G. Farquharson, and S. J. Frasier, 2004: Initial vector velocity estimates from the UMass Dual Beam Interferometer. *Igarss 2004: Ieee*



International Geoscience and Remote Sensing Symposium Proceedings, Vols 1-7, 976-979.

Toporkov, J. V., D. Perkovic, G. Farquharson, M. A. Sletten, and S. J. Frasier, 2005: Sea surface velocity vector retrieval using dual-beam interferometry: First demonstration. *Ieee Transactions on Geoscience and Remote Sensing*, 43, 2494-2502.

Toporkov, J. V., P. A. Hwang, M. A. Sletten, S. J. Frasier, G. Farquharson, and D. Perkovic, 2010: Observation of a Boat and Its Wake with a Dual-Beam Along-Track Interferometric Sar. *2010 Ieee International Geoscience and Remote Sensing Symposium*, 1940-1943.

Toporkov, J. V., P. A. Hwang, M. A. Sletten, G. Farquharson, D. Perkovic, and S. J. Frasier, 2011: Surface Velocity Profiles in a Vessel's Turbulent Wake Observed by a Dual-Beam Along-Track Interferometric SAR. *Ieee Geoscience and Remote Sensing Letters*, 8, 602-606.

Voronovich, A. G., and V. U. Zavorotny, 2011, Depolarization of microwave backscattering from a rough sea surface: modeling with small-slope approximation. *IGARSS 2011*, 24-29 July 2011, Vancouver, Canada, 2033-2036.